



Contents lists available at ScienceDirect

Engineering Science and Technology, an International Journal

journal homepage: www.elsevier.com/locate/jestch



An innovative architecture of a three-speed automatic internal shifting hub for regular commuting bicycles: Kinematic analysis and preliminary sizing

Lorenzo Pagliari, Chiara Nezzi, Renato Vidoni, Franco Concli*

Faculty of Science and Technology, Free University of Bolzano, Piazza Università 1, 39100 Bolzano, Italy



ARTICLE INFO

Keywords:

Shifting hub system
Bicycle
Automatic internal shifting hub
Gear ratio
Kinematic analysis
Driving cycle
Planetary gears

ABSTRACT

Bicycle transmission systems represent a key component in the design of bicycles, as they determine the nature of pedaling effort that riders have to provide. Multi-gear systems enable riders to choose between multiple transmission ratios and are typically divided into external and internal. The present work aims at designing a three-speed automatic internal shifting hub for regular (non-electric) bicycles, starting from an already existing alternative with only two gear ratios (i.e., speeds), which is taken as reference. The complete kinematic design and a preliminary dimensioning are implemented and described in detail. The novelty of the design lays in the number of available gear ratios (three), which is an unprecedented result for automatic internal shifting hubs for regular bicycles, as it is unmatched by the models available on the market. The higher number of gear ratios increases the number of available combinations of torque and pedaling cadence to achieve a certain velocity, granting more riding flexibility and ultimately enabling easier rides. This is proven through validation by numerical simulation of a driving cycle, which shows that lower and more constant pedaling forces are required when using the novel three-speed automatic internal shifting hub with respect to the two-speed reference model.

1. Introduction and background

1.1. Bicycles transmission systems

Due to the current climate change issues humanity is facing, bicycles are becoming an increasingly popular mean of transportation for emissions reduction purposes [1,2]. Studies and academic research on bicycles have been developed and published, e.g., comparing bicycles cost with cars [3] or dealing with the role of bicycles in urban traffic [4]. The interest in their analysis is proved by the numerous and diverse articles analyzing their dynamics, modelling, and design [5–8]. In this regard, their transmission system represents a crucial component [9–11]. Although various examples in literature deal with different types of bicycles, from traditional to electric ones, the scope of this section is to briefly review existing typologies of transmission systems for only regular (i.e., non-electric) bicycles.

Bicycles transmission systems can be divided into two groups: external changing-speed and internal multi-speed systems [12]. The former typology is also named “derailleur system” and is a system consisting of a chain, multiple sprockets, and the derailleur, a chain-guide mechanism that moves the chain from one sprocket to another

[13], offering different speed ratios for different situations on a multi-speed bicycle [14–16]. Due to the lack of external protection of their components from potential impacts and the diagonal alignment of the chain while shifting from most of the gears, derailleur systems are characterized by a higher need for maintenance [17], if compared to internal shifting hub systems. Internal shifting hub systems were introduced at the beginning of the 20th century. In 1901, Archer invented a mechanism which allowed the rider to change speed while riding [18]. This mechanism provided three different speeds, hence the cyclist could choose freely between low, high, normal, and “free wheel”. In the following years, bicycle parts manufacturers, like Shimano, SRAM, Sturmey Archer and Fichtel & Sachs AG have researched and developed their own internal shifting hubs. Taking a closer look to the internal shifting hub system architecture, the possibility to have different speed ratios is guaranteed by the use of a planetary gear mechanism [19], which is connected through a chain to the chainring, which is attached to the pedals. Planetary gears grant high efficiency, large reduction ratios, compactness, high transmittable power density [20,21], and torques [22], making them employed for an extremely wide range of industries, e.g., automotive [22], aerospace [23], and power generation applications [24], such as wind energy production [25,26]. A complete description of the components of conventional internal shifting hubs can

* Corresponding author.

E-mail address: franco.concli@unibz.it (F. Concli).

Nomenclature	
a	Bicycle acceleration
A_F	Frontal area
C	Maximum pedaling cadence
C_{AS}	Torque provided by the cyclist, TSAISH
C_{AX}	Torque provided by the cyclist, SRAM Automatix
C_D	drag coefficient
$d_{P,RG}$	Ring gear pitch diameter, TSAISH
$F_{N,G1}$	Normal force when first gear is engaged, TSAISH
$F_{N,G3}$	Normal force when third gear is engaged, TSAISH
f_R	Rolling friction coefficient between bicycle tire and road
$F_{R,G1}$	Radial force when first gear is engaged, TSAISH
$F_{R,G3}$	Radial force when third gear is engaged, TSAISH
$F_{T,G1}$	Tangential force when first gear is engaged, TSAISH
$F_{T,G3}$	Tangential force when third gear is engaged, TSAISH
g	Gravitational acceleration
$i_{ext,AS}$	External transmission ratio, TSAISH
$i_{ext,AX}$	External transmission ratio, SRAM Automatix
$i_{int,AS,G1}$	First gear internal transmission ratio, SRAM Automatix
$i_{int,AS,G2}$	Second gear internal transmission ratio, SRAM Automatix
$i_{int,AS,G3}$	Third gear internal transmission ratio, SRAM Automatix
$i_{int,AS,GX}$	internal transmission ratio according to bicycle velocity at each timestep, TSAISH
$i_{int,AX,G1}$	First gear internal transmission ratio, SRAM Automatix
$i_{int,AX,G2}$	Second gear internal transmission ratio, SRAM Automatix
$i_{int,AX,GX}$	internal transmission ratio according to bicycle velocity at each timestep, SRAM Automatix
m	Gears module
m_{CB}	Mass of cyclist plus bicycle
n_p	Number of planets of planetary gearing
P	Wheel perimeter
P_D	Power to be supplied due to drag resistance
P_I	Power to be supplied due to inertial forces
P_{RF}	Power to be supplied due to friction forces
P_T	Power to be supplied at each driving cycle time step
r_s	Sun gear radius
v	Bicycle velocity
$V_{AX,G1,90}$	Bicycle velocity at maximum cadence when first gear is engaged, SRAM Automatix
$V_{AX,G2,90}$	Bicycle velocity at maximum cadence when second gear is engaged, SRAM Automatix
$V_{AS,G1,90}$	Bicycle velocity at maximum cadence when first gear is engaged, TSAISH
$V_{AS,G2,90}$	Bicycle velocity at maximum cadence when second gear is engaged, TSAISH
$V_{AS,G3,90}$	Bicycle velocity at maximum cadence when third gear is engaged, TSAISH
Z_P	Planet gears teeth number, TSAISH
Z_{RG}	Ring gear teeth number, TSAISH
Z_S	Sun gear teeth number, TSAISH
α	Pressure angle
η_C	Bicycle chain efficiency
η_T	Shifting hub efficiency
ρ	Density of the air at standard conditions
τ_{crank}	Torque at the crankshaft
$\tau_{crank,AS}$	Torque at the crankshaft, TSAISH
$\tau_{crank,AX}$	Torque at the crankshaft, SRAM Automatix
$\tau_{PC,G3}$	Torque at the planetary carrier gear when third gear is engaged
$\tau_{RG,G1}$	Torque at the ring gear when first gear is engaged
$\tau_{spr,48,17}$	Torque at the sprocket with a 48 teeth chainring and a 17 teeth sprocket
$\tau_{SG,G1}$	Torque at the sun gear when first gear is engaged
$\tau_{SG,G3}$	Torque at the sun gear when third gear is engaged
$\tau_{spr,max}$	Maximum torque at the sprocket
τ_w	Torque at the wheel
ω_{PC}	Planetary carrier gear rotational speed, TSAISH
ω_{RG}	Ring gear rotational speed, TSAISH
ω_S	Sun gear rotational speed, TSAISH
ω_w	Wheel angular velocity

be found in [27]. The main advantages with respect to derailleur systems are the protection from external impacts and dirt, and a better chain alignment. This results in less maintenance and a higher reliability [13] and represents a significant advantage in the case of city and tourism bikes. On the contrary, when race bikes are concerned, lightness is more important than maintenance, derailleur systems are always preferred.

Despite the broad availability of the two systems, single-speed road bicycles are very popular in cities thanks to their ease of use (no speed shift is performed), little need for maintenance, lower price and ruggedness. However as soon as there are gradients, or empty streets, the single-speed becomes a major drawback [28]: accelerating, climbing and maximum speed are compromised due to the single gear ratio. A compromise can be found using an automatic internal shifting hub, which enables to drive with different transmission ratios, while still granting ease of use, since shifts are automatically changed depending on the angular velocity of the hub [29]. Automatic multi-speed internal shifting hubs can be divided into electric and a mechanical. In the first case the shift control mechanism is represented by a controller which compares the sensed speed to the speed range stored in the controller memory for a specific gear position of the bicycle [30] and gives this information to an actuator that modifies the gear position accordingly. In the second case, the shift is actuated automatically in relation to the rotation of the hub components by making use of control devices such as centrifugal clutches, centrifugal governors and sprag clutches [31]. Depending on the speed change, a centrifugal clutch pushes or draws the shifting control device and hence actuates the automatic shift.

Centrifugal governors operate in a similar way with respect to centrifugal clutches. The basic functioning principle of centrifugal governors is based on the exploitation of the centrifugal force acting on two masses, which control a sensing element and can govern it thanks to their centrifugal movement [32]. Eventually, sprag clutches allow a single direction of rotation for the free wheel mode, but produce binding if the torque is applied in the other direction [33]. The main purpose of exploiting sprag clutches is indeed their high suitability for free wheel pedaling, since they allow a relative motion free of any resistance in one single direction of rotation.

In conclusion, automatic internal shifting hubs represent one of the latest and most innovative solutions for bicycles transmission systems, solving various problems of previous and simpler variants. Their common application is however conceived for electric bicycles, and few solutions are present on the market for regular bicycles, as it is shown by the next chapter.

1.2. Market analysis

This section offers an insight into the typologies of automatic internal shifting hubs available on the market. For this reason, a brief market research was conducted. Factors like brand and model, adaptability, number of stages, gear ratios, and weight are used as dividers. What comes to light is that available automatic internal shifting hubs are suitable for electric bicycles only. The sole type of automatic shifting hub adaptive to regular bicycles is the one produced by SRAM, as

reported in Table 1 [34].

The SRAM Automatix can shift between a neutral gear (gear ratio of 1) and overdrive (gear ratio of 1.36) based on the angular velocity of the bicycle wheel. It needs to be stated that the gear ratio range provided by SRAM Automatix is somehow limited and a solution with three gear ratios would for sure be preferred. Many examples in literature, indeed, highlight that 3-speed transmission systems offer a potentially perfect combination of system simplicity but also adaptability to different pedaling conditions [38]. For this reason, a further market research was conducted where, the analysis was focused on existing internal shifting hubs with three gear ratios (Table 2), which were surely developed on the basis of the well-known patent by James Archer [18]. It results indeed important to review also non-automatic internal shifting hubs present on the market, whose properties could be used for the future development of this work. The research was limited to three-speed internal shifting hubs, on which the work of this paper will subsequently be focused. The analysis led to the identification of models produced by Shimano and SRAM, which are listed among the top 5 Tier-1 manufacturers of bicycle components aftermarket [39]. For sake of completeness, additional typologies by Sturmey-Archer are included, as it results to offer the widest selection of three-speed non-automatic internal shifting hubs nowadays [40]. For this second market research, factors like brand and model, mechanism, number of stages, gear ratios, and weight were used as dividers. It needs to be stated that three-speed internal shifting hubs represent a limited part of the current market offer. Bicycle parts manufacturers have indeed switched to solutions with numbers of gear ratios higher than 10. As said, it is however obvious that many of the currently available internal shifting hubs with up to three gears are based on the principle of the cross shaped clutch in combination with planet stages, first patented by Archer [18], resulting in a reliable and diffused solution.

1.3. Aim and novelty of the work

As investigated, automatic shifting hub solutions are currently not so widespread or common on the market. An interesting example was developed by Hsieh et al. [52] but it is thought for a direct application on electric assisted bicycles, which goes beyond the scope of this work. Given the previous market analyses, it goes without saying that the unique option of automatic internal shifting hub for regular bicycles is represented by the SRAM Automatix [34], which is characterized only by two gear ratios. Since examples with a higher number of gear ratios are still missing in literature, scholars intend to give their contribution to this topic through the development of an automatic internal shifting hub for regular bikes, characterized by three available gears, and therefore named Three-Speed Automatic Internal Shifting Hub (TSAISH). Therefore, the SRAM Automatix is taken as reference model, whose performance should be improved through the design of the new shifting hub described in this article by increasing the number of available gears from two to three. This is the key point where the novelty of the TSAISH architecture lays. Adopting three gear ratios instead of two increases the number of available combinations of torque and pedaling cadence to achieve a certain velocity, ensuring more riding flexibility and enabling

Table 1
Market search on automatic internal gear hubs.

Brand and Model	Adaptability	N° stages	Gear ratios	Weight [g]
SRAM Automatix [34]	Regular bicycles	2	1—1.36	780
Shimano Nexus Inter-5E [35]	Electric bicycles	5	1—1.277—1.622 —2.07—2.63	1650
Enviolo Automatiq [36]	Electric bicycles	∞	0.5 ÷ 1.9	Not available
Bafang GHA-3 [37]	Electric bicycles	3	1—1.36—1.65	1700

Table 2

Market search on internal gear hubs.

Brand and Model	Type of mechanism	N° stages	Gear ratios	Weight [g]
Shimano Nexus 3 SG-3D55 [41]	Cross Shaped Clutch axially actuated	3	0.623—0.741—1	945
Shimano Nexus 3 SG-3C41 [42]	Cross Shaped Clutch axially actuated	3	0.73—1—1.36	1120
Shimano Nexus 3 SG-3R75-B [43]	Cross Shaped Clutch axially actuated	3	0.632—0.741—1	1315
SRAM i-motion 3 [44]	Cross Shaped Clutch axially actuated	3	0.73—1—1.36	1120
Sturmey Archer S-RF3 [45]	Cross Shaped Clutch axially actuated	3	0.75—1—1.33	970
Sturmey Archer SX-RB3 [46]	Cross Shaped Clutch axially actuated	3	0.75—1—1.33	1240
Sturmey Archer SX-RK3 [47]	Cross Shaped Clutch axially actuated	3	0.75—1—1.33	1400
Sturmey Archer S-RC3 [48]	Cross Shaped Clutch axially actuated	3	0.75—1—1.33	1290
Sturmey Archer S-RK3 [49]	Cross Shaped Clutch axially actuated	3	0.75—1—1.33	1080
Sturmey Archer RS-RF3 [50]	Cross Shaped Clutch axially actuated (with rotary gear selector)	3	0.75—1—1.33	990
Sturmey Archer RX-RD3 [51]	Cross Shaped Clutch axially actuated (with rotary gear selector)	3	0.75—1—1.33	1440

easier rides at lower and medium velocities, while granting to reach the same top velocities (when the highest gear is engaged) of the SRAM Automatix. As far as the functional design of the TSAISH is concerned, the shifting hub will be completely characterized from a kinematic point of view, while regarding its dimensioning, a preliminary sizing of the hub gears will be presented. Since, as it will be later illustrated, multiple characteristics of the proposed design will be conceived starting from those of the SRAM Automatix, a real-world model of such shifting hub has been analyzed and, through a reverse-engineering process, all its geometrical features have been measured.

This paper will be structured as follows: first, the design of the TSAISH is discussed in Section 2. Thereafter, the preliminary sizing of the gearing components will be described in Section 3. The validation of the developed design is presented in Section 4, where the performance of the TSAISH and of the SRAM Automatix are compared over a driving cycle. Eventually, the key results of the design phase are summarized, and the remarkable characteristics of the final solution for the developed automatic internal gear hub are highlighted. Finally, conclusions and future work are drawn.

2. Shifting hub design

2.1. Calculation of desired gear ratios

The first step for the design of the TSAISH is the definition of the desired three gear ratios that have to be achieved. Indeed, once a maximum pedaling cadence is fixed, the gear ratios that will be chosen will determine the maximum reachable bicycle velocity when each of the three gears is engaged, impacting on the range of bicycle velocities that can be achieved. Some assumptions and boundary conditions have to be fixed, in order to calculate the three desired gear ratios of the TSAISH. Such boundary conditions are:

- the dimensions of the bicycle wheel, which is assumed to be a 700C type wheel, one of the most common and widespread models [53]. Such wheel is characterized by a 622 mm diameter rim and a 25 mm wide tire [54];
- the type of tire that is mounted on the selected wheel, which is assumed to respect the European Tyre and Rim Technical Organization (ETRTO) standards [55], hence having an external perimeter (P) of 2135 mm;
- the maximum pedaling cadence that is reached while commuting (C), which is set to 90 rpm. This value is recommended as optimal cadence for professional cyclists during prolonged cycling [56], making it a reasonable value as maximum cadence for a normal commuter;
- the target maximum bicycle velocity that is reached while cycling at maximum cadence, with the highest TSAISH gear engaged, which is fixed at 44 km/h. This is the round value of the maximum bicycle velocity that is reached while cycling at maximum cadence and the highest SRAM Automatix gear engaged, as will be later proved. If the maximum bicycle velocity achieved when the highest gear is engaged is the same for both the TSAISH and the SRAM Automatix, by providing the TSAISH with three gears instead of two the same velocities spectrum is covered by more gears, and granting a higher riding flexibility and ease to the cyclist;
- the difference in percentage of the transmission ratio value between each of the three gears, which is set similar to that of the SRAM Automatix, at 45 %. This means that when the third gear is engaged, the transmission ratio is 45 % higher than that of the second gear, and when the second gear is engaged, the transmission ratio is 45 % higher than that of the first gear.

Once these boundary conditions are set, it is possible to define the three desired gear ratios that the automatic shifting hub should achieve to improve the cycling experience with respect to the SRAM Automatix. Since in this section multiple transmission ratios will be mentioned, in order not to get confused while dealing with them from this point on the following nomenclature is introduced:

- when referring to any gear ratio characterizing a transmission stage taking place outside the shifting hub, such ratio will be called “external” and will be assigned with the label “ext”. This is the case of the transmission stage between the bicycle chainring and the sprocket.
- when referring to any gear ratio characterizing a transmission stage taking place inside the shifting hub, such ratio will be called “internal” and will be assigned with the label “int”.

If the SRAM Automatix is employed, at the maximum cadence of 90 rpm the device works with the second gear engaged (transmission ratio $i_{int,AX,G2} = 1.36$). Assigning the chainring and the sprocket with 48 and 17 teeth respectively (one of the most common and widespread solutions [57]), the external transmission ratio, between chainring and sprocket, is:

$$i_{ext,AX} = 48t/17t = 2.82 \quad (1)$$

As a result, the achievable ($V_{AX,G2,90}$) and the achievable bicycle velocity at maximum cadence when the first gear ($i_{int,AX,G1} = 1$) is engaged ($V_{AX,G1,90}$) are:

$$V_{AX,G2,90} = C \bullet P \bullet i_{ext,AX} \bullet i_{int,AX,G2} = 44.2 \text{ km/h} \quad (2)$$

$$V_{AX,G1,90} = C \bullet P \bullet i_{ext,AX} \bullet i_{int,AX,G1} = 32.5 \text{ km/h} \quad (3)$$

If the three-gear automatic internal shifting hub is employed, considering that the target maximum bicycle velocity of 44 km/h is achieved when the third gear is engaged, the target maximum velocities achieved when the second and the first gear are engaged can be calculated by recalling that the transmission ratio increase from one gear to the following one has been fixed to 45 %:

$$V_{AS,G3,90} = C \bullet P \bullet i_{ext,AS} \bullet i_{int,AS,G3} = 44.0 \text{ km/h} \quad (4)$$

$$V_{AS,G2,90} = C \bullet P \bullet i_{ext,AS} \bullet i_{int,AS,G2} = 31.4 \text{ km/h} \quad (5)$$

$$V_{AS,G1,90} = C \bullet P \bullet i_{ext,AS} \bullet i_{int,AS,G1} = 22.4 \text{ km/h} \quad (6)$$

where $i_{ext,AS}$ is the external transmission ratio of the TSAISH, while $i_{int,AS,G1}$, $i_{int,AS,G2}$, and $i_{int,AS,G3}$ are the three gear ratios to be selected. Note that both the external and the internal gear ratios are to be defined, as they both influence the transmission of power from the pedals to the bicycle rear wheel. However, the external gear ratio is fixed and does not change with the bicycle velocity, as it is determined by the number of chainring and sprocket teeth. Only the internal gear ratio changes (according to the values that are selected for $i_{int,AS,G1}$, $i_{int,AS,G2}$, and $i_{int,AS,G3}$) and produces a change in the transmission of power. As a result, the external gear ratio (which can be easily modulated just by installing different chainrings or sprockets) will be calculated only after the internal gear ratios that most facilitate the design of the TSAISH will have been selected.

There is an infinite number of triads of internal transmission ratios that satisfies the condition of increasing of 45 % from one gear to the following one. However, if it is set that for one of the three transmission stages a direct gear is employed, meaning that in one case the sprocket and hub shell (i.e., the wheel) rotate at the same angular velocity, then the number of triads of internal transmission ratios is reduced to three. Each one of the three triads (Series 1, Series 2, and Series 3, shown in Table 3) display one ratio equal to 1, which corresponds to the transmission ratio of a direct gear. The use of a direct gear is introduced to perform one of the three transmission stages in the simplest possible way, through a direct connection between the sprocket and the hub shell and decreasing the complexity, weight, and volume of the automatic shifting hub.

In Series 1 the direct connection between sprocket and hub shell is achieved when the low gear ($i_{int,AS,G1}$) is engaged. In this case the largest transmission ratios are achieved and in particular $i_{int,AS,G3}$ exceeds 2. As a result, a single planetary gear stage with a fixed sun gear is not suitable [58], and a more sophisticated approach is required, increasing the complexity, weight, and volume of the automatic shifting hub. In Series 2 the direct connection between sprocket and hub shell is achieved when the neutral gear ($i_{int,AS,G2}$) is engaged. This is the same solution adopted in James Archer's patent [18], where, when the neutral gear is engaged, the sprocket drives the planetary ring gear, which directly drives the hub shell, bypassing the planetary gear stage. In Series 3 the direct

Table 3
TSAISH potential triads of internal transmission ratios.

	$i_{int,AS,G1}$	$i_{int,AS,G2}$	$i_{int,AS,G3}$
Series 1	1	1.45	2.105
Series 2	0.69	1	1.45
Series 3	0.475	0.69	1

connection between sprocket and hub shell is achieved when the high gear ($i_{int,AS,G3}$) is engaged. In this case the largest transmission ratios are achieved. The use of two reductions increases the complexity of the hub design. Each one of the three Series is taken into account in the definition process of the best configuration of the three-gear automatic internal shifting hub.

2.2. TSAISH configuration

The limitations which characterize the combinations of gear ratios of Series 1 and Series 3, and which have been described above, cause the discard of all the potential designs based on them, as they compromise the simplicity, lightness and realizability of the TSAISH. As a result, the configuration which best meets such characteristics, and which is proposed in this article, is based on Series 2, resulting in a configuration similar to that of the Sturmey Archer hub [18], with both configurations making use of a single stage planetary transmission with a fixed sun gear and with same input and output paths. However, it must be reminded that despite the similarity, the Sturmey Archer hub is a three-speed internal shifting hub, while the device presented in this article is a TSAISH. Such difference is achieved by employing a mechanism to change gear that relies on a combination of ratchet freewheels and centrifugal clutches.

The functioning of freewheels is not affected by the angular velocity of the hub. They have the task of granting the transmission of torque between driveshaft and driven shaft unless the driven shaft velocity is higher than that of the driveshaft, in which case they are disengaged, overrunning the freewheel. The disengagement that is provided by ratcheting mechanisms allow riders to coast, i.e., to stop pedaling while the bicycle is still in forward motion. If no freewheel were employed, the chainring would be never disengaged from the rear wheel hub and the pedals would keep rotating whenever the bicycle is in motion. As far as the clutches are concerned, their functioning does depend on the angular velocity of the hub. They are designed so that when the bicycle accelerates and a certain angular velocity value is reached, the centrifugal forces which are involved are enough to activate the clutch mechanism and engage the drive shaft with the driven shaft. Of course, if the velocity decreases, and the centrifugal forces are no longer enough, the centrifugal clutches disengage. Also in the case of the centrifugal clutches ratchet mechanisms represent a valid solution and are employed for the design of the TSAISH. The mechanism scheme and the section of the draft of the TSAISH are represented in Fig. 1 and Fig. 2 respectively.

Let us analyze how each gear ratio is obtained and what path is followed by the power in each case:

- $i_{int,AS,G1}$: the lowest transmission ratio is achieved when the angular velocity of the rear wheel (hence the bicycle velocity) is low, meaning that Clutch 1 and Clutch 2 are disengaged since the centrifugal forces are not large enough. The ring gear is employed as power input and the planet carrier as power output (Fig. 3). The sprocket carrier drives the ring gear via Freewheel 1, and the ring gear drives the planet carrier via the planetary stage (note that being an epicyclic gearing with fixed sun gear, planetary carrier and ring gear have equal direction of rotation). The planet carrier is connected to the hub shell through Freewheel 2, transferring the power to the wheel.
- $i_{int,AS,G2}$: the neutral transmission ratio is achieved at $V_{AS,G1,90}$, when the velocity is enough to cause Clutch 1 to engage, connecting the sprocket directly to the planet carrier, which works now as power input. The planet carrier is directly connected to the shell hub through Freewheel 2, transferring the torque without making use of the planetary transmission stage (Fig. 4). Freewheel 1 is overrun, as the ring gear already rotates with its final relative velocity. The planet carrier therefore works also as power output.
- $i_{int,AS,G3}$: the highest transmission ratio is achieved at $V_{AS,G2,90}$, when the velocity is enough to engage Clutch 2, connecting the ring gear to the hub shell. The sprocket is still connected to the planet carrier through Clutch 1, which works as input shaft and transfers the torque to the ring gear, which is used as power output (Fig. 5). Freewheel 2 is now also overrun and the transfer of the torque occurs only by the two engaged clutches.

Note that the two clutches are positioned on the drivetrain, which during coasting is disengaged from the hub shell (and therefore, from the rear wheel), as the freewheels are overrun. This means that every time the cycler coasts, the clutches are not directly influenced by the rotational speed of the wheel, and they experience no centrifugal forces. As a result, they will return to their initial state and the hub automatically shifts down to the first gear. However, this does not represent a problem for the function of the TSAISH. Indeed, as the rider starts pedaling again, the drivetrain is accelerated until it matches the angular velocity the hub shell, and the clutches engage again at their specified shift points even before the drivetrain is transferring power to the wheel. The components which comprise the freewheels and the clutches and which allow them to be engaged, disengaged, or overrun will be described in Chapter 3, which deals with the sizing of the elements comprising the TSAISH. The gears and the corresponding states of clutches and freewheels are reported in Table 4.

2.3. Teeth selection and transmission ratios verification

As stated above, the desired increase between each value of the in-

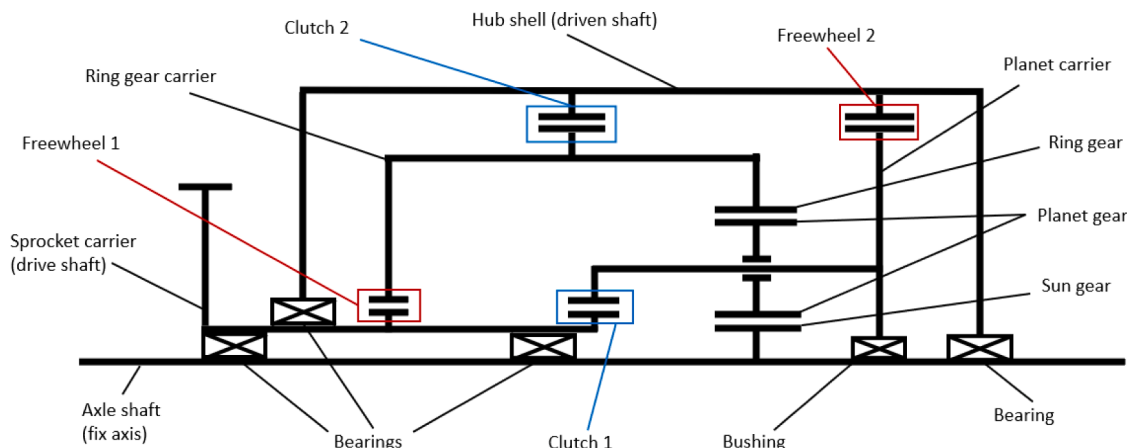


Fig. 1. TSAISH kinematic scheme.

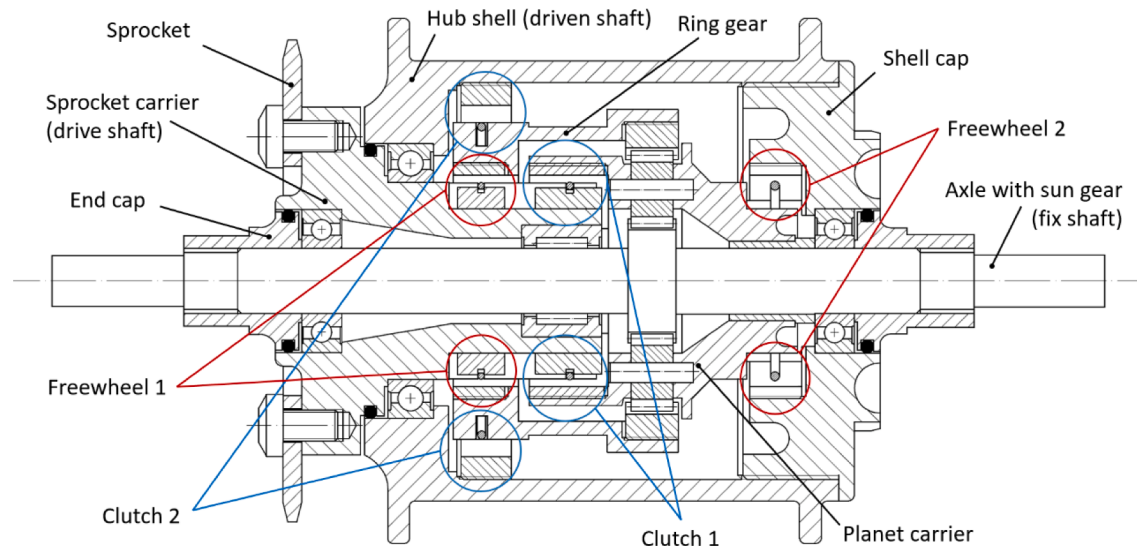


Fig. 2. TSAISH draft section.

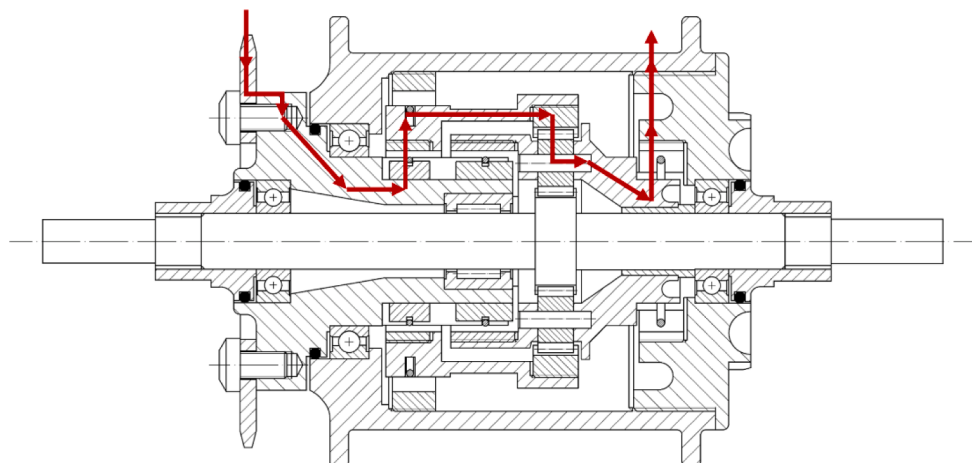


Fig. 3. Power path when the first gear is engaged.

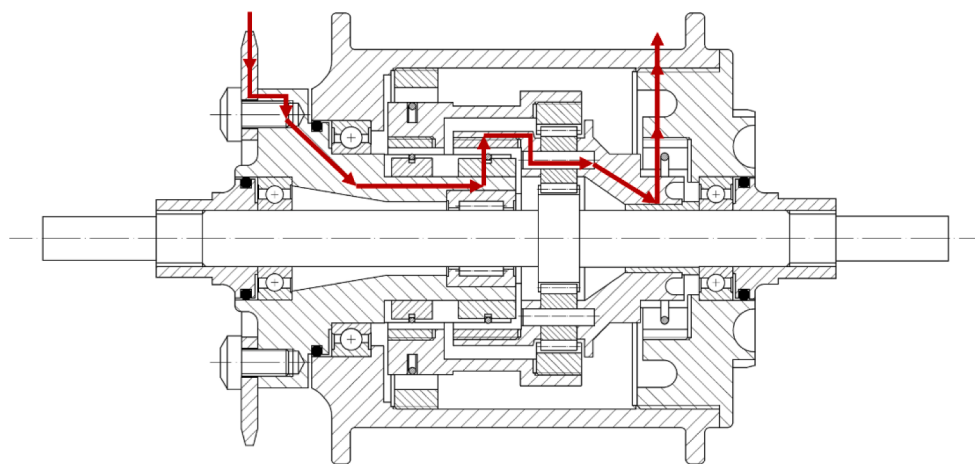


Fig. 4. Power path when the second gear is engaged.

ternal transmission ratios is of 45 %. However, the increase that is actually achieved depends on the number of teeth that is selected for the ring gear (z_{RG}), the planets (z_p) and the sun gear (z_S). Such choice is

made taking into account that z_{RG} is directly linked to the outer dimensions of the planetary gearing. Selecting a value for z_{RG} that is too high would imply an excessively bulky shifting hub device. Considering

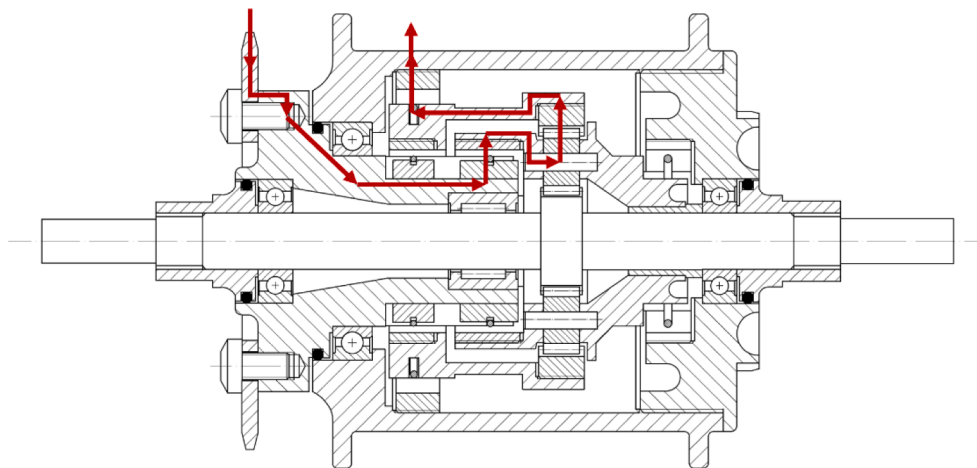


Fig. 5. Power path when the third gear is engaged.

Table 4
Operation of each of the TSAISH gear clutches and freewheels.

Gear	Clutch 1	Clutch 2	Freewheel 1	Freewheel 2	Power input	Power output
$i_{int,AS,G1}$	Disengaged	Disengaged	Engaged	Engaged	Ring gear	Planet carrier
$i_{int,AS,G2}$	Engaged	Disengaged	Engaged	Overrun	Planet carrier	Planet carrier
$i_{int,AS,G3}$	Engaged	Engaged	Overrun	Overrun	Planet carrier	Ring gear

that in the case of the SRAM Automatix the ring gear pitch circle has a diameter of 37.6 mm and taking such measure as reference dimension to have a sufficiently compact shifting hub, the configuration that allows to have a ring gear pitch circle diameter as close as possible to the reference dimension, while granting a percentage increase of the transmission ratio value between each of the three gears as close as possible to 45 % is the following:

- a sun gear with 20 teeth, $z_S = 20$;
- planets with 15 teeth, $z_P = 15$;
- a ring gear with 50 teeth, $z_{RG} = 50$.

With such teeth number, and assuming a module equal to that of the SRAM Automatix ($m = 0.8 \text{ mm}$), the resulting ring gear pitch diameter is:

$$d_{P,RG} = m \cdot z_{RG} = 40 \text{ mm} \quad (7)$$

Considering, for a preliminary rough sizing, the module of the TSAISH equal to that of the SRAM Automatic represents a reasonable assumption, because, as presented in Section 3.1, given a torque at the sprocket, the loads experienced by the planetary components of both shifting hubs are very similar. Once z_{RG} , z_P and z_S are selected, fixed a unitary angular velocity for the input shaft, the first and third gear ratios can be calculated through the relations binding the relative velocities in a planetary gearing. In particular, when the first gear is engaged the ring gear works as input shaft and the planet carrier works as output shaft ($\omega_{RG} = 1$, $\omega_S = 0$), therefore:

$$i_{int,AS,G1} = (\omega_{RG} \cdot z_{RG} - \omega_S \cdot z_S) / (z_{RG} + z_S) = 0.71 \quad (8)$$

When the third gear is engaged, the planet carrier works as input shaft and the ring gear as output shaft ($\omega_{PC} = 1$, $\omega_S = 0$), therefore:

$$i_{int,AS,G3} = \omega_{PC} \cdot (z_{RG} - z_S) - (\omega_S \cdot z_S / z_{RG}) = 1.4 \quad (9)$$

The resulting increase in gear ratio that is obtained is of 41 % between $i_{int,AS,G2}$ and $i_{int,AS,G1}$, and of 40 % between $i_{int,AS,G3}$ and $i_{int,AS,G2}$ (Table 5).

Assuming $i_{ext,AS}$ to have equal value of $i_{ext,AX}$ (obtained by assigning the chainring and the sprocket with 48 and 17 teeth respectively), the

Table 5
TSAISH actual transmission ratios.

Gear	Value	Increase from previous value
$i_{int,AS,G1}$	0.71	–
$i_{int,AS,G2}$	1	41 %
$i_{int,AS,G3}$	1.4	40 %

maximum velocities that are reached with a cadence of 90 rpm for each of the three gears are:

$$V_{AS,G3,90} = C \cdot P \cdot i_{ext,AS} \cdot i_{int,AS,G3} = 44.6 \text{ km/h} \quad (10)$$

$$V_{AS,G2,90} = C \cdot P \cdot i_{ext,AS} \cdot i_{int,AS,G2} = 31.8 \text{ km/h} \quad (11)$$

$$V_{AS,G1,90} = C \cdot P \cdot i_{ext,AS} \cdot i_{int,AS,G1} = 22.6 \text{ km/h} \quad (12)$$

3. TSAISH rough sizing

3.1. Forces determination

To dimension the components comprising the TSAISH, it is fundamental to define the forces and torques that they transmit. A bicycle hub has to withstand a wide range of different load conditions that heavily depend on the riding style, terrain and weight of the cyclist, which represent complex data that are often not made available by manufacturers. However, the norm ISO 4210-8:2014 [59] provides a set of loads which can be employed to replicate the loading conditions that a bicycle experiences and to size its components. In particular, according to ISO 4210-8:2014 the drivetrain components of a bicycle have to be able to withstand a static force of 1500 N applied at the center of the leading pedal with the cranks in horizontal position. Assuming a crank length of 175 mm (one of the most common and widespread solutions [60]), such force produces a torque of 263 Nm at the crankshaft (τ_{crank}). Depending on the size of the chainring, the resulting chain tension varies. If a 48 teeth chainring and a 17 teeth sprocket are employed (external gear ratio $i_{ext,AS} = 2.82$) the torque at the sprocket is:

$$\tau_{spr,48,17} = \tau_{crank}/i_{ext,AS} = 93.3 \text{ Nm} \quad (13)$$

However, more critical conditions could be reached if a chainring and sprocket characterized by a smaller transmission ratio were employed, since the resulting torque at the sprocket would be higher than $\tau_{spr,48,17}$. In particular, the smallest transmission ratio achievable with regular components is of 1.9, as recommended by manufacturers [61]. As a result, the highest achievable torque at the sprocket, $\tau_{spr,max}$ is:

$$\tau_{spr,max} = \tau_{crank}/1.9 = 138.4 \text{ Nm} \quad (14)$$

The ISO 4219–8:2014 static test is conceived to be representative of a scenario where the first gear is engaged and the first instants of bicycle acceleration after stand still are taken into account, when the peak torque values in the drivetrain are reached. Instead, when the two higher gears are engaged, the involved torques have to be derived from the maximum human power output that is provided by the rider. However, according to [62], which analyzed the torques developed by elite cyclists, even in cases of gears different from the first one, torque values higher than 250 Nm at the crank are not even reached by professionals in a competitive race environment. Such value is lower than that of the torque τ_{crank} that was obtained above, considering a force of 1500 N applied at the crank, and consequently, the torque at the hub $\tau_{spr,max}$ seems to be a reasonable option to be employed as design torque for the sizing of the three-speed internal automatic shifting hub. Moreover, to size with an additional degree of safety, $\tau_{spr,max}$ is rounded to 150 Nm in the sizing procedure.

3.2. Planetary sizing

Once the maximum torque acting on the sprocket ($\tau_{spr,max} = 150 \text{ Nm}$) is defined, the first dimensioning step that is taken is to size the spur gears of the planetary gearing, which is done by determining the highest load conditions that they experience (i.e., the conditions where the forces acting on their teeth are maximum) and selecting the right teeth geometry accordingly, through the procedures prescribed by the ISO 6336 standard [63]. As a consequence, there are two transmission configurations to be considered: when the first gear is engaged (when power is transmitted from the ring gear to the planet carrier) and when the third gear is engaged (when power is transmitted from the planet carrier to the ring gear). The transmission of power when the second gear is engaged is a scenario that is not relevant for the design of the planetary, as in this case forces are transmitted directly from the sprocket carrier via the planet carrier to the hub shell, without actively passing through the planet stage. Ring gear and planets rotate with the planet carrier but do not transfer power.

To determine the worst loading condition between the two configurations mentioned above, a typical number of three planets ($n_p = 3$), and a pressure angle of $\alpha = 25^\circ$ (a commonly used value in power transmitting gears [64]) are assumed, and the torques and forces that take place in the planetary gearing (Fig. 6) are calculated for each configuration:

- when the first gear is engaged, the ring is directly connected to the sprocket (i.e., the torque at the ring gear $\tau_{RG,G1}$ is equal to that at the sprocket, 150 Nm) and transmits the power with ratio $i_{int,AS,G1}$ to the three planets, whose carrier is connected to the hub. In this case, the tangential ($F_{T,G1}$), radial ($F_{R,G1}$), and normal ($F_{N,G1}$) forces that are exchanged are:

$$F_{T,G1} = \tau_{SG,G1}/(n_p \bullet r_s) = 2500 \text{ N} \quad (15)$$

$$F_{R,G1} = F_{T,G1} \bullet \tan(\alpha) = 1166 \text{ N} \quad (16)$$

$$F_{N,G1} = \sqrt{(F_{T,G1})^2 + (F_{R,G1})^2} = 2759 \text{ N} \quad (17)$$

where r_s is the sun gear radius (it can be calculated using m and z_S), and

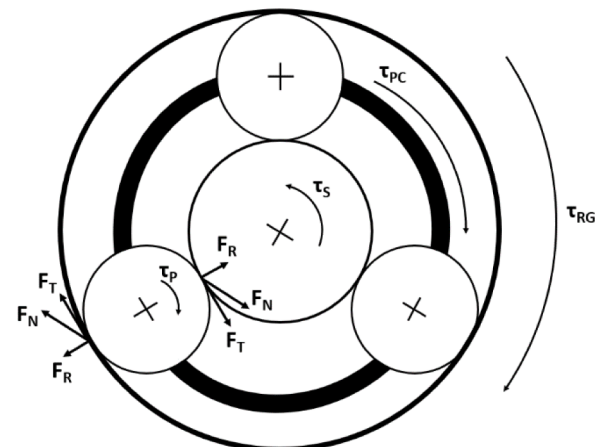


Fig. 6. Torques and forces exchanged in the planetary gearing. Forces are represented for one planet only.

$\tau_{S,G1}$ is the torque at the sun gear when the first gear is engaged (calculated as $\tau_{SG,G1} = \tau_{RG,G1} \cdot z_S/z_{RG}$).

- when the third gear is engaged, the planet carrier is directly connected to the sprocket (i.e., the torque at the planet carrier $\tau_{PC,G3}$ is 150 Nm) and transmits the power to the ring gear, which is connected to the hub. In this case, the tangential ($F_{T,G3}$), radial ($F_{R,G3}$), and normal ($F_{N,G3}$) forces that are exchanged are:

$$F_{T,G3} = \tau_{SG,G3}/(n_p \bullet r_s) = 1792 \text{ N} \quad (18)$$

$$F_{R,G3} = F_{T,G3} \bullet \tan(\alpha) = 863 \text{ N} \quad (19)$$

$$F_{N,G3} = \sqrt{(F_{T,G3})^2 + (F_{R,G3})^2} = 1977 \text{ N} \quad (20)$$

where $\tau_{S,G3}$ is the torque at the sun gear when the third gear is engaged and can be calculated as $\tau_{SG,G3} = \tau_{RG,G3} \cdot (z_S/z_{RG})$, and $\tau_{RG,G3}$ is the torque at the ring gear when the third gear is engaged, equal to $\tau_{RG,G3} = \tau_{PC,G3} \cdot (z_{RG}/(z_{RG} + z_s))$.

The first configuration, with the first gear engaged, displays higher tangential, normal, and radial forces, resulting the highest load condition. Note that since the planetary gearing is characterized by three symmetrically arranged planets, the net radial force on the axle and the ring gear is zero. If the same calculations are repeated with the SRAM Automatix data (teeth number, module, pressure angle, number of planets), when the second gear is engaged and same torque at the sprocket is considered, very similar, slightly smaller, loads than those obtained in the first configuration are found.

Using the loads obtained in the first configuration, the planetary gearing components are sized through gear-sizing software which integrates the dimensioning procedure prescribed by the ISO 6336 standard. The boundary conditions that are inserted in the software are those set until now, plus a condition on the gearing material and one of failure probability:

- module $m = 0.8 \text{ mm}$, as that of the SRAM Automatix, as they experience very similar loads when the same torque is applied at the sprocket;
- pressure angle $\alpha = 25^\circ$;
- teeth numbers $z_S = 20$, $z_P = 15$, $z_{RG} = 50$;
- number of planets $n_p = 3$;
- forces corresponding to those identified by the highest load condition determined above;
- gearings made of 18CrNiMo7;
- failure probability equal or lower of that obtained with the geometry of the SRAM Automatix.

The resulting geometry which best satisfies these conditions is characterized by a width of 6.7 mm (0.4 mm wider than that of the SRAM Automatix).

4. Validation

In this section, a validation of the design discussed up to now is presented. The validation is carried out through numerical analysis, by calculating the torques and the pedaling cadence that have to be supplied during a driving cycle and by comparing those obtained when the SRAM Automatix is employed to those obtained when the TSAISH is employed. Since standard driving cycles for bicycles do not exist, a driving cycle experimentally developed [65] is taken into account (Fig. 7). The cycle was developed for an electric bike, and it is representative of an urban environment, featuring frequent accelerations and decelerations. Starting from the driving cycle data, namely, the bicycle velocity (v) corresponding to each timestep comprising the cycle, the acceleration (a) can be found as the derivative of the velocities. As far as the terrain slope is concerned, since this project focuses on urban environments, flat terrain is assumed for the whole cycle. The power that is supplied by the cyclist at each timestep of the driving cycle is calculated as:

$$P_T = (P_I + P_{RF} + P_D)/(\eta_C + \eta_T) \quad (21)$$

where P_I is the power needed to overcome the inertial forces, P_{RF} is power needed to overcome the rolling friction forces, and P_D is the power needed to overcome the drag resistance. η_C is the bicycle chain efficiency and is assumed to be 0.99 [66] for a chain transmission with 48 teeth at the drive sprocket and 17 teeth at the driven sprocket (like the one employed for the kinematic design described above). η_T is the shifting hub efficiency and is assumed to be 0.98 for both the SRAM Automatix and the TSAISH, a reasonable value for planetary gearings employed in in-hub bicycle transmission [67]. P_I is:

$$P_I = m_{CB} \bullet a \bullet v \quad (22)$$

where m_{CB} is the mass of the cyclist plus that of bicycle and it is assumed to be 92 kg (80 kg for the cyclist and 12 kg for the bicycle). P_{RF} is calculated as:

$$P_{RF} = m_{CB} \bullet g \bullet f_R \bullet v \quad (23)$$

where $g = 9.81 \text{ m/s}^2$ is the gravitational acceleration and f_R is the rolling friction coefficient between bicycle tire and road (fixed at 0.0077, as typical value for regular commuters [68]). P_D , assuming no wind effect, is computed as:

$$P_D = 0.5 \bullet \rho \bullet C_D \bullet A_F \bullet v^3 \quad (24)$$

where $\rho = 1.2 \text{ kg/m}^3$ is the density of air at 101325 Pa and 293.25 K, while C_D (unit-less), and A_F (in m^2) are respectively the drag coefficient and the frontal area of the cyclist plus the bicycle. For the product $C_D \cdot A_F$ the value of 0.559 m^2 can be taken when for regular commuters are

considered [68]. With the parameters assumed above, P_T is calculated for each timestep, with an average of the overall cycle of 132.2 W. Once P_T is known, the torque at the wheel (τ_W) for each second of the cycle is found as:

$$\tau_W = P_T / \omega_W \quad (25)$$

where ω_W is the wheel angular velocity, calculated as $\omega_W = v/P \cdot 2\pi$. As far as the TSAISH is concerned, the torque at the crankshaft provided by the cyclist is:

$$\tau_{crank,AS} = \tau_W \bullet i_{ext,AS} \bullet i_{int,AS,GX} \quad (26)$$

where $i_{ext,AS} = 2.82$ (48 teeth at the chairing and 17 teeth at the sprocket) and where $i_{int,AS,GX}$ is the internal transmission ratio that the TSAISH provides according to the bicycle velocity at each timestep (namely, it can be equal to $i_{int,AS,G1} = 0.71$, $i_{int,AS,G2} = 1$ or $i_{int,AS,G3} = 1.4$). As far as the SRAM Automatix is concerned, the torque at the crankshaft provided by the cyclist is:

$$\tau_{crank,AX} = \tau_W \bullet i_{ext,AX} \bullet i_{int,AX,GX} \quad (27)$$

where $i_{ext,AX} = 2.82$ and where $i_{int,AX,GX}$ is the internal transmission ratio that the SRAM Automatix provides according to the bicycle velocity at each timestep (namely, it can be equal to $i_{int,AX,G1} = 1$, $i_{int,AS,G2} = 1.36$). With regard to the pedaling cadence (which corresponds to the crankshaft angular velocity) it is calculated (in rpm) for the TSAISH (C_{AS}) and for the SRAM Automatix (C_{AX}) respectively as:

$$C_{AS} = (\omega_W / i_{ext,AS}) \bullet i_{int,AS,GX} \bullet (60/2\pi) \quad (28)$$

$$C_{AX} = (\omega_W / i_{ext,AX}) \bullet i_{int,AX,GX} \bullet (60/2\pi) \quad (29)$$

The torques and pedaling cadence that the cyclist provides throughout the overall cycle in the case the SRAM Automatix and in the case TSAISH is employed are represented in Fig. 8. Significant parameters obtained from the numerical analysis are reported in Table 6, where a comparison between the two shifting hub is proposed. From the numerical analysis it emerges that during the simulated driving cycle, thanks to the additional speed that the TSAISH makes available with respect to the SRAM Automatix, the cyclist rides applying a lower and more constant torque, while working at higher pedaling cadences. More in detail, the average torque (calculated by not considering all the timesteps where there is deceleration, and therefore zero torque is applied to the pedals), the maximum torque and the standard deviation of the torques decrease of 26.9 %, 18.2 % and 22.9 % respectively. The first two results indicate that thanks to the additional speed of the TSAISH (especially the lowest one, $i_{int,AS,G1} = 0.71$) the cyclist is generally required to apply a lower force on the pedals. The third result suggests that not only the pedaling torque throughout the driving cycle is lower, but also that it is applied in a more constant manner.

With regard to the pedaling cadence, the average cadence, the maximum cadence and the standard deviation of the cycle cadences, they are higher when the TSAISH is employed. This is a normal outcome consequent to the fact that the power input necessary to ride at the

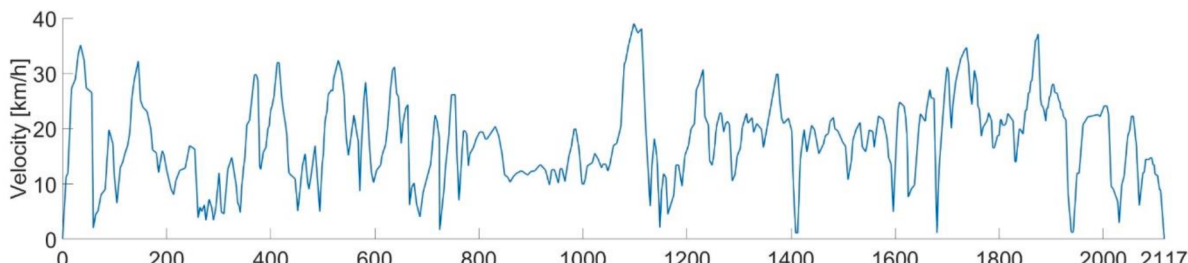


Fig. 7. Velocity versus time diagram of the driving cycle employed for the validation.

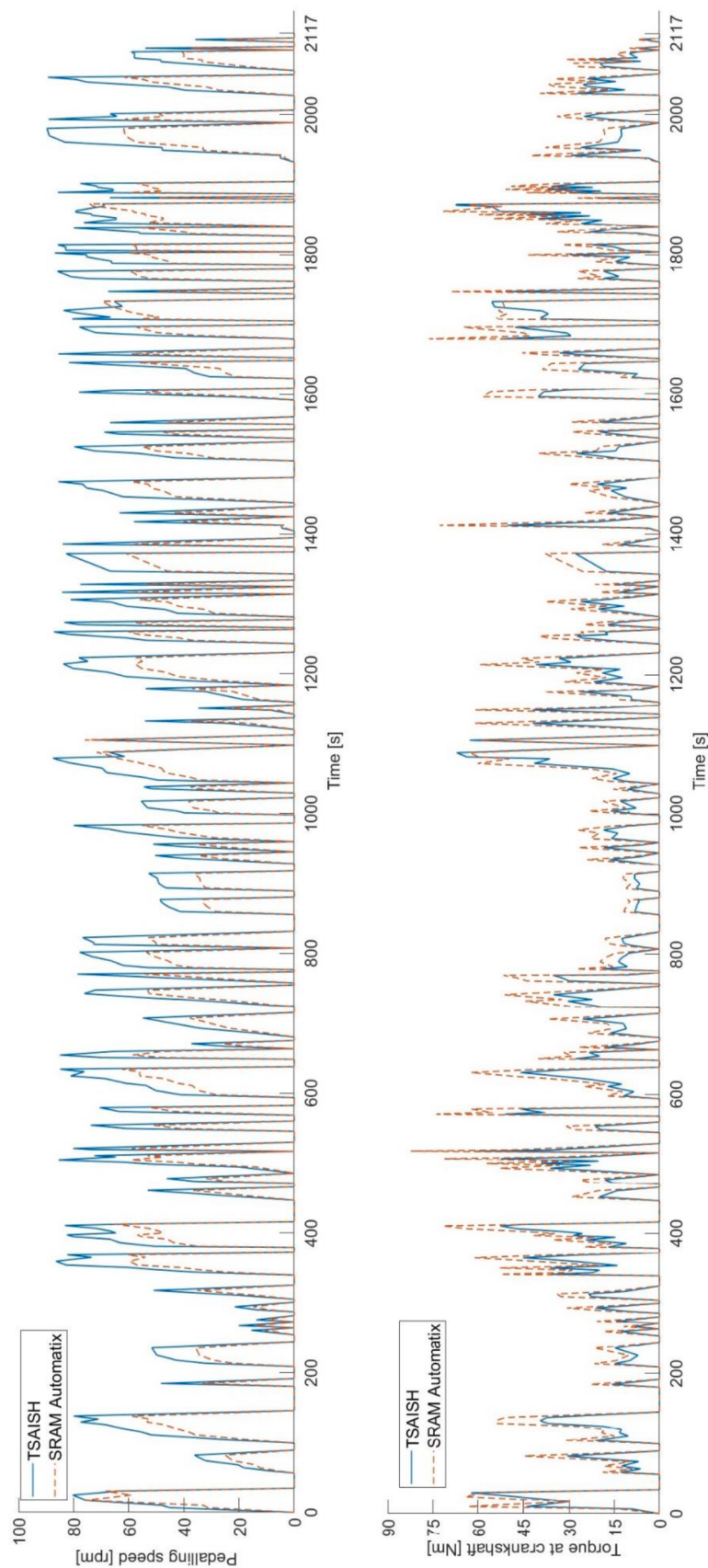


Fig. 8. Pedaling speed and instantaneous torques at the crankshaft when the TSAISH (continuous line) and the SRAM Automatix (dotted line) are employed.

Table 6

Driving cycle parameters comparison, SRAM Automatix vs TSAISH.

Parameter	SRAM Automatix	TSAISH	Variation
Average torque	33.2 Nm	24.1 Nm	- 26.9 %
Maximum torque	82.3 Nm	67.3 Nm	- 18.2 %
Torques standard deviation	20.3	15.7	- 22.9 %
Average pedaling cadence	42.1 rpm	58.5 rpm	+ 39.1 %
Maximum pedaling cadence	76 rpm	89.6 rpm	+ 19 %
Pedaling cadence standard deviation	24.1	33	+ 37.1 %

velocities prescribed by the driving cycle is always the same at each timestep, both when the SRAM Automatix and the TSAISH are employed. If the torques are generally lower when the TSAISH is considered, then inevitably the pedaling cadences must increase to provide the same power input. Nevertheless, the pedaling cadence never exceeds the maximum value set above of 90 rpm. What defines an improved riding easiness remains the fact that the torque, and therefore the force the cyclist has to exert on the pedals, is lower and more homogenous. As a result, the validation confirms the advantages the TSAISH can provide.

Eventually, a brief commentary should be added regarding the maximum torque to be provided during the driving cycle, which is 82.3 Nm in the case of the SRAM Automatix and 67.3 Nm in the case of the TSAISH. The two torques correspond to a force at the pedal (considering a crank length of 175 mm, as above) of about 48 kg and 39 kg respectively. To explain the high intensity of such forces, it has to be taken into account that they are applied only in a timestep where it is required a high acceleration from standstill, because the driving cycle requires the cyclist to stop (for example to respect a red traffic light or to let a pedestrian cross the road) and to depart again. In such situation, it has to be considered that the cyclist can exert such high forces on the pedals by using their own bodyweight. In light of this, the forces obtained above result reasonably manageable by a cyclist with a bodyweight of 80 kg, as assumed for the simulation.

For sure, further validation of the design scheme is required and a wide experimental campaign is intended to be carried out by the authors. Finite Element Analysis and bench tests are necessary to perform a detail sizing of the TSAISH, especially with regard to the shifting hub axle, the bearings, the sprocket carrier and the hub shell. Moreover, they can be exploited to characterize the power losses of the shifting hub. Finite Element Analysis can be employed to also optimize the structural properties of the TSAISH architecture, while optimizing its weight.

5. Conclusions

The TSAISH represents a novel example of architecture of automatic internal shifting hub for regular bicycles. After researching the current market, it emerges that the only established model of such devices is the SRAM Automatix, which is taken as reference model for the development of the TSAISH. The TSAISH is designed so that it features three different gear ratios, an unprecedented number for automatic internal shifting hubs for regular bicycles, and one more with respect to the reference model. A higher number of gears increases the number of combinations of torque and pedaling cadence to achieve a certain velocity, providing cyclists with more riding flexibility. In this regard, a validation is carried out through numerical analysis of the torque and pedaling cadence that are applied during a driving cycle, comparing the values that are obtained when the TSAISH and the SRAM Automatix are employed. Results show that the TSAISH enables cyclists to ride by applying lower and more regular forces on the pedals with respect to the SRAM Automatix. In this regard, it has also to be said that the structural complexity of the TSAISH architecture is higher than that of the SRAM Automatix and other common internal shifting hubs, with potential drawbacks on reliability and costs. However, as far as reliability is concerned, it is pointed out that the TSAISH is designed for regular

bicycles rather than for race or sport bicycles. Therefore, it is conceived for commuting in urban environments, without undergoing large loads, repeated shocks, and without operating in environments characterized by significant quantities of dirt or mud. As a result, once the shifting hub is properly manufactured and assembled, following all required quality standards, its higher complexity does represent a significant reliability issue with respect to similar shifting hubs. As far as production costs are concerned, the higher complexity of the TSAISH causes them to increase, especially if few components are produced. However, through mass production also a complex device such as the TSAISH can be manufactured maintaining low and competitive costs. In addition, the higher performance in terms of riding easiness and flexibility makes it market-competitive even if its costs are higher than other shifting hubs. In addition to the kinematic design, a rough sizing of the TSAISH is carried out, providing a preliminary identification of the main dimensions characterizing its components. A limitation of the current work is the preliminary nature of the TSAISH sizing, and therefore future developments and further validation is intended by the author, in particular through Finite Element Analysis and bench tests, which will provide the required information for a fine sizing, weight and performance optimization.

Declaration of competing interest

The authors declare that they have no known competing financial interests or personal relationships that could have appeared to influence the work reported in this paper.

References

- [1] A. Doria, E. Marconi, L. Munoz, A. Polanco, D. Suarez, An experimental-numerical method for the prediction of on-road comfort city bicycles, *Veh. Syst. Dyn.* 59 (9) (2021) 1376–1396.
- [2] S. Klug, A. Moja, A. Verhagen, D. Görges, S. Savarese, The influence of bicycle fork bending on brake control, *Veh. Syst. Dyn.* (2019) 1–21.
- [3] S. Gössling, A.S. Choi, Transport transitions in Copenhagen: comparing the cost of cars and bicycles, *Ecol. Econ.* 113 (2015) 106–113.
- [4] H. Twaddle, T. Schendzielorz, O. Fakler, Bicycles in urban areas: review of existing methods for modeling behavior, *Transp. Res. Rec.* 2434 (1) (2014) 140–146.
- [5] A. Doria, S.D. Roa Melo, On the influence of tyre and structural properties on the stability of bicycles, *Veh. Syst. Dyn.* 56 (6) (2018) 947–966.
- [6] Pradhan, T.R., Sunil, D.A., Shrivastava, A., 2023. Static Structural Analysis of Bike Suspension System. Available at SSRN 4563828.
- [7] N. Tomiati, G. Magnani, M. Marcon, An experimental investigation of the bicycle motion during a hands-on shimmy, *Veh. Syst. Dyn.* 59 (9) (2021) 1443–1459.
- [8] J. Veeraragu, V.R. Mula, Improving ride dynamics of bicycle using negative stiffness-based suspension in low-frequency vibration region. *Advances in simulation, Prod. Des. Dev.* (2022) 53–65.
- [9] P. Wang, J. Yi, T. Liu, Stability and control of a rider-bicycle system: analysis and experiments, *IEEE Trans. Autom. Sci. Eng.* 17 (1) (2019) 348–360.
- [10] Q. Ge, Q. Sun, S.E. Li, S. Zheng, W. Wu, X. Chen, Numerically stable dynamic bicycle model for discrete-time control, *IEEE Intelligent Vehicles Symposium Workshops 2021* (2021) 128–134.
- [11] Billianto, K., et al., 2020. Strength analysis for designing a bicycle transmission system without chain. *IOP Conference Series: Materials Science and Engineering*, 1007.
- [12] T.H. Chen, L.C. Hsieh, On the design and prototype manufacturing of multi-speed transmission device of bicycle, *MATEC Web of Conferences, EDP Sciences* 185 (2018).
- [13] Y.C. Wu, L.A. Chen, Design of an 8-speed internal gear hub with a rotary control mechanism for bicycles, *Tehnički Vjesnik-Technical Gazette* 22 (4) (2015) 865–871.
- [14] G. Dinesh, Design and Structural Analysis of a Bicycle Frame Under Static Loading Conditions, Andhra University, 2022. Doctoral dissertation.
- [15] T.Y. Lin, C.H. Tseng, An experimental approach characterizing rear bicycle derailleur systems. Part I: performance test, *Int. J. Veh. Des.* 19 (3) (1998) 356–370.
- [16] T.Y. Lin, C.H. Tseng, An experimental approach characterizing rear bicycle derailleur systems. Part II: the stability region and its applications, *Int. J. Veh. Des.* 19 (3) (1998) 371–384.
- [17] Colegrave, J., Dylan, H., Gonzalez, S., 2010. Bicycle rear wheel suspension system. United States Patent No. US 7,837,213 B2.
- [18] Archer, J., 1902. Variable gearing for velocipedes and road motor-vehicles. United States Patent No. US 753,785 A.
- [19] F. Concli, Low-loss gears precision planetary gearboxes: reduction of the load dependent power losses and efficiency estimation through a hybrid analytical-numerical optimization tool, *Forsch. Ingenieurwes.* 81 (2017) 395–407.

- [20] L. Macchioni, Y. Borgianni, F. Concli, High power density speed reducers: a TRIZ based classification of mechanical solutions, IFIP Advances in Information and Communication Technology 597 (2020) 243–253.
- [21] L. Macchioni, F. Concli, M. Blagojevic, A new three-stage gearbox concept for high reduction ratios: use of a nested-cycloidal architecture to increase the power density, Mech. Mach. Theory 181 (2023).
- [22] F. Chaari, M.S. Abbes, F.V. Rueda, A.F. del Rincon, M. Haddar, Analysis of planetary gear transmission in non-stationary operations, Front. Mech. Eng. 8 (1) (2012) 88–94.
- [23] M. Iglesias, A. Fernandez, A. De-Juan, R. Sancibrian, P. Garcia, Planet position errors in planetary transmission: effect on load sharing and transmission error, Front. Mech. Eng. 8 (1) (2013) 80–87.
- [24] X. Yu, Y. Huangfu, Y. Yang, M. Du, Q. He, Z. Peng, Gear fault diagnosis using gear meshing stiffness identified by gearbox housing vibration signals, Front. Mech. Eng. 17 (4) (2022) 57.
- [25] Y.S. Sun, S.R. Yu, S.X. Li, Y.N. He, Review of the damage mechanism in wind turbine gearbox bearings under rolling contact fatigue, Front. Mech. Eng. 14 (4) (2019) 434–441.
- [26] P. Yi, L. Dong, T. Shi, Multi-objective generic algorithms based structural optimization and experimental investigation of the planet carrier in wind turbine gearbox, Front. Mech. Eng. 17 (4) (2022) 57.
- [27] Matsueda, K., Tanaka, K., 2006. Bicycle internal gear shifting hub. United States Patent No. US 7,148,582 B2.
- [28] M.T. Lebec, C. Kortny, D. Baumgartel, Overuse injuries associated with mountain biking: is single-speed riding a predisposing factor? Sports 2 (1) (2014) 1–13.
- [29] Okochi, H., 2003. Internal transmission device with automatic shift mechanism for a bicycle. United States Patent No. US 6,558,288 B2.
- [30] Jordan, B.T., 2002. Automatic bicycle shifting system. United States Patent No. US 2002/0094906, 1002-07-18.
- [31] Hsieh, L.C., Chen, T.H., 2011. The systematic design of multi-speed internal gear hub for a bicycle. Advanced Materials Research, Trans Tech Publications Ltd, 199.
- [32] Zanto, R., 2014. Automatic two-speed fixed-drive bicycle hub-gear. Diss. University of Cincinnati, College of Engineering and Applied Science.
- [33] D.J. Olinger, J. Goela, Performance characteristics of a 1 kw scale kite-powered system, J. Sol. Energy Eng. 132 (2019) 4.
- [34] SRAM Automatix. User Manual, Publ. No. 95-3315-001-000 Rev. A, SRAM LLC, 2011.
- [35] Automatic internal gear hub for electric bikes Shimano Nexus Inter-5E. User Manual, SHIMANO INC. ITP, November 2022.
- [36] Automatic internal gear hub for electric bikes Enviolo Automatiq. Technical Manual CY, enviolo, May 2022.
- [37] The new Bafang 3-Speed Automatic Gear Hub (GHA-3). User Manual, Bafang Electric (Suzhou) Co. Ltd., July 2022.
- [38] E.A. Casteel, M. Archibald, A study on the efficiency of bicycle hub gears. ASME international mechanical engineering congress and exposition, Am. Soc. Mech. Eng. 56420 (2013).
- [39] Bicycle Components Aftermarket Outlook (2022-2032). Report, Publ. No. REP-GB-5829, Future Market Insights Inc., July 2022.
- [40] 3-speed internal gear hubs. Product Catalogue 2017-2018, Sun Race Sturmey-Archer Inc, 2018.
- [41] SHIMANO NEXUS Internal Geared Hub Disc Brake 3-speed. User Manual, SHIMANO INC. ITP, July 2021.
- [42] SHIMANO NEXUS Internal Geared Hub Coaster Brake 3-speed. User Manual, SHIMANO INC. ITP, July 2022.
- [43] SHIMANO NEXUS Internal Geared Hub Rolle Brake 3-speed. User Manual, SHIMANO INC. ITP, January 2022.
- [44] Sram i-motion 3. User Manual, Publ. No. 5300 E/D/F/Nl/Dk/Sv, SRAM Corporation, June 2006.
- [45] Sturmey-Archer 3 Speed Freewheel Rear Hub S-RF3. Product Catalogue 2017-2018, Sun Race Sturmey-Archer Inc, 2018.
- [46] Sturmey-Archer 3 Speed Band Brake Rear Cruiser Hub SXRB3. Product Catalogue 2017-2018, Sun Race Sturmey-Archer Inc, 2018.
- [47] Sturmey-Archer 3 Speed Disc Brake Rear Cruiser Hub SXRK3. Product Catalogue 2017-2018, Sun Race Sturmey-Archer Inc, 2018.
- [48] Sturmey-Archer 3 Speed Coaster Brake Rear Hub S-RC3. Product Catalogue 2017-2018, Sun Race Sturmey-Archer Inc, 2018.
- [49] Sturmey-Archer 3 Speed Disc Brake Rear Hub S-RK3. Product Catalogue 2017-2018, Sun Race Sturmey-Archer Inc, 2018.
- [50] Sturmey-Archer 3 Speed Freewheel Rear Hub RS-RF3. Product Catalogue 2017-2018, Sun Race Sturmey-Archer Inc, 2018.
- [51] Sturmey-Archer 3 Speed 70mm Drum Brake Rear Hub. Product Catalogue 2017-2018, Sun Race Sturmey-Archer Inc, 2018.
- [52] Hsieh, L.C., Chen, T.H., 2008. The Systematic Design of Automatic Three-speed Gear Hub for Bicycles. Proceedings of the International Multiconference of Engineers and Computer Scientists, 2.
- [53] J. Forester, Effective cycling, 6th ed, MIT Press, Boston, 1992.
- [54] C.B. Puig, Recumbent bicycle design, Universitat Politècnica de Catalunya, 2014. BS thesis.
- [55] Tyre designations and dimensions for Bicycle tyres and rims. ISO Technical standard 31/SC 10/WG 16, 2021.
- [56] C.R. Abbis, P. Laursen, J.J. Peiffer, Optimal cadence selection during cycling, International SportMed Journal 1 (2009).
- [57] A. Becker, Mathematics and explanatory generality, Philisophia Mathematica 25 (2017) 2.
- [58] L.C. Hsieh, H.C. Tang, The kinematics of eight-speed planetary gear hubs for bicycles, Appl. Mech. Mater. 232 (2012).
- [59] International Organization for Standardization, ISO 4210-8:2014, Cycles, Safety requirements for bicycles, Part 8: Pedal and drive system test methods, 2014.
- [60] O. Inbar, R. Dotan, T. Trousil, Z. Dvir, The effect of bicycle crank-length variation upon power performance, Ergonomics 26 (1983).
- [61] Rohloff SPEEDHUB 500/14. Handbook: Technical data, Rohloff AG, 2022.
- [62] A.S. Gardner, J.C. Martin, D.T. Martin, M. Barras, D.G. Jenkins, Maximal torque-and power-pedaling rate relationships for elite sprint cyclists in laboratory and field tests, Springer Verlag 101 (3) (2007) 287–292.
- [63] International Organization for Standardization, ISO 6336:2019, Calculation of load capacity of spur and helical gears, 2019.
- [64] M.V. Murali, S.L. Ajit Prasad, Influence of module and pressure angle on contact stresses in spur gears, International Journal of Mechanical Engineering and Robotics Research 5 (2016) 3.
- [65] Savadi, T., Abhilash, V.N., Fernandes, K., Patil, S.S., 2022. Development of a Drive Cycle and Resultant Powertrain Calculations of Electric Bicycle. Recent Advances in Hybrid and Electric Automotive Technologies.
- [66] N.E. Hollingworth, D.A. Hills, Theoretical efficiency of a cranked link chain drive, Proceedings of the Institution of Mechanical Engineers, Part C 200 (1986) 375–377.
- [67] Y.C. Wu, C.H. Cheng, Computing the power flow and mechanical efficiency of in-hub bicycle transmissions, Eng. Comput. 31 (2014) 2.
- [68] S. Tengattini, A.Y. Bigazzi, Physical characteristics and resistance parameters of typical urban cyclists, Journal of Sport Sciences 36 (20) (2018) 2383–2391.